Naturally occurring branched-chain polyamines induce a crosslinked meshwork structure in a giant DNA

Akira Muramatsu, Yuta Shimizu, Yuko Yoshikawa, Wakao Fukuda, Naoki Umezawa, Yuhei Horai, Tsunehiko Higuchi, Shinsuke Fujiwara, Tadayuki Imanaka, and Kenichi Yoshikawa

Citation: J. Chem. Phys. **145**, 235103 (2016); doi: 10.1063/1.4972066

View online: http://dx.doi.org/10.1063/1.4972066

View Table of Contents: http://aip.scitation.org/toc/jcp/145/23

Published by the American Institute of Physics

Naturally occurring branched-chain polyamines induce a crosslinked meshwork structure in a giant DNA

Akira Muramatsu,[1] Yuta Shimizu,[1] Yuko Yoshikawa,[1] Wakao Fukuda,[2] Naoki Umezawa,[3,a)] Yuhei Horai,[3] Tsunehiko Higuchi,[3] Shinsuke Fujiwara,[4] Tadayuki Imanaka,[2] and Kenichi Yoshikawa[1,a)]

[1]*Faculty of Life and Medical Sciences, Doshisha University, Kyotanabe 610-0394, Japan*
[2]*College of Life Sciences, Ritsumeikan University, Kusatsu 525-8577, Japan*
[3]*Graduate School of Pharmaceutical Sciences, Nagoya City University, Nagoya 467-8603, Japan*
[4]*School of Science and Technology, Kwansei-Gakuin University, Sanda 669-1337, Japan*

(Received 24 September 2016; accepted 29 November 2016; published online 19 December 2016)

We studied the effect of branched-chain polyamines on the folding transition of genome-sized DNA molecules in aqueous solution by the use of single-molecule observation with fluorescence microcopy. Detailed morphological features of polyamine/DNA complexes were characterized by atomic force microscopy (AFM). The AFM observations indicated that branched-chain polyamines tend to induce a characteristic change in the higher-order structure of DNA by forming bridges or crosslinks between the segments of a DNA molecule. In contrast, natural linear-chain polyamines cause a parallel alignment between DNA segments. Circular dichroism measurements revealed that branched-chain polyamines induce the A-form in the secondary structure of DNA, while linear-chain polyamines have only a minimum effect. This large difference in the effects of branched- and linear-chain polyamines is discussed in relation to the difference in the manner of binding of these polyamines to negatively charged double-stranded DNA. [http://dx.doi.org/10.1063/1.4972066]

I. INTRODUCTION

Polyamines, small cationic compounds with two or more amino groups, are found in all living cells and play roles in cell growth, proliferation, and many other important cellular functions.[1] The most common natural polyamines are putrescine [2+], spermidine [3+], and spermine [4+], all of which have a linear skeleton. It is known that these polyamines affect the induction of DNA condensation/compaction.[2–8] Since genomic DNA is often found in a hierarchically condensed structure, this may contribute to gene regulation.[9] It has been reported that spermine [4+] is much more potent at promoting DNA compaction than putrescine [2+] and spermidine [3+], which indicates that the valence strongly influences the degree of DNA compaction.[5,10–13] In addition to the number of positive charges, structural differences also affect their interactions with DNA. Several systematic studies have shown that their influence on DNA compaction is dependent on the geometrical arrangement of positively charged amino groups.[7,14–20] It has been reported that the potential for DNA compaction exhibits an even-odd effect with respect to the number of methylene groups that separate neighboring amino groups.[15,21] Chiral effects on DNA compaction have also been reported.[22,23]

To date, a large number of studies have examined the condensation/compaction of DNA.[11–13,15,17,18,24–33] Bloomfield, a pioneer in the field of DNA condensation, stated that "generally, the term "condensation" is reserved for situations in which the aggregate is of finite size and orderly morphology."[24] In many previous reports, DNA condensation was often interpreted as a highly cooperative binding phenomenon, i.e., the transition to induce condensation was regarded as a mixed process that included aggregation, shrinkage, compaction, and precipitation. About two decades ago, the compaction of single DNA molecules was found to be an essentially all-or-none process based on a real-time single-molecule observation by fluorescence microscopy (FM).[34] It was also found that some condensing agents induce only loosely shrunken states that are markedly different from DNA compaction.[35,36] As for the folding transition of giant DNA into a tightly compact state, i.e., DNA compaction, it has become clear that the density of DNA segments in the compact state is 10^4-10^5 times higher than that in the elongated conformation at the level of single DNA molecules.[27] Such characteristics of an all-or-none transition are only seen for giant DNA molecules above the size of several kilobase pairs. It was reported that giant DNA molecules in a swollen state tend to exhibit highly parallel ordering on a 2D surface just before full compaction under the addition of spermidine [3+].[37] In contrast, short fragmented DNA molecules on the size of kilobase pairs only show a random arrangement under similar concentrations of spermidine.[37]

Recently, it was found that thermophilic microorganisms synthesize longer- and/or branched-chain polyamines.[38–41] These unique polyamines are expected to play an important role in maintaining genetic activities at high temperatures.

a)Authors to whom correspondence should be addressed. Electronic addresses: umezawa@phar.nagoya-cu.ac.jp and keyoshik@mail.doshisha.ac.jp

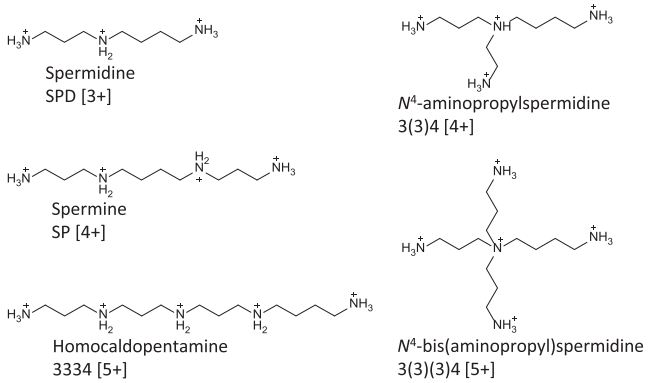

SCHEME 1. Structures of linear- and branched-chain polyamines examined in this study.

In this study, we evaluated the structural effects of tetra- and pentavalent branched-chain polyamines, N^4-aminopropylspermidine [3(3)4] and N^4-bis(aminopropyl)spermidine [3(3)(3)4], on the higher-order structure of DNA in comparison with those of spermidine, spermine, and homocaldopentamine [3334] (see chemical structures in Scheme 1). These unique branched-chain polyamines, 3(3)4 and 3(3)(3)4, are found in a hyperthermophilic archaeon organism, *Thermococcus kodakarensis*. To visualize and characterize the large-scale conformational transition of DNA at the single-molecule level, we used T4 GT7 phage DNA (166 kbp, 57 μm) as a model for large DNA and monitored the folding process by fluorescence microscopy (FM) and atomic force microscopy (AFM). We also investigated the effects of these polyamines on the secondary structure of DNA by circular dichroism (CD). The resulting DNA/polyamine complex structures are discussed in relation to the difference in the nature of the interaction of linear- and branched-chain polyamines with DNA.

II. EXPERIMENTAL

A. Materials

Spermidine [SPD] and spermine [SP] were purchased from Nacalai Tesque (Kyoto, Japan). N^4-aminopropylspermidine [3(3)4], homocaldopentamine [3334] and N^4-bis(aminopropyl)spermidine [3(3)(3)4] were synthesized as described in the supplementary material. Calf Thymus DNA (CT DNA: 8-15 kbp) was purchased from Sigma-Aldrich (St. Louis, MO, USA). T4 GT7 phage DNA was purchased from Nippon Gene (Toyama, Japan). The fluorescent cyanine dye YOYO-1 (1,1′-(4,4,8,8-tetramethyl-4,8-diazaundecamethylene)bis[4-[(3-methylbenzo-1,3-oxazol-2-yl)methylidene]-l,4-dihydroquinolinium]tetraiodide) was purchased from Molecular Probes, Inc. (Eugene, OR, USA). The antioxidant 2-mercaptoethanol (2-ME) was purchased from Wako Pure Chemical Industries (Osaka, Japan). Other chemicals were analytical grade and also obtained from commercial sources.

B. Direct observation of the higher-order structure of DNA in bulk solution by FM

T4 phage DNA was dissolved in a 10 mM Tris-HCl buffer and 4%(v/v) 2-ME at *p*H 7.5 in the presence of various concentrations of polyamines (0–3000 μM). Measurements were conducted at a low DNA concentration (0.1 μM in nucleotide units). To visualize individual DNA molecules by FM, 0.05 μM of YOYO-1 (Excitation/Emission 491/509 nm) was added to the DNA solution. Single-molecule observations were performed with an Axiovert 200 inverted fluorescence microscope (Carl Zeiss, Oberkochen, Germany) equipped with a 100× oil-immersion objective lens and fluorescent illumination from a mercury lamp (100 W) via a filter set (Zeiss-10, excitation BP 450-490; beam splitter FT 510; emission BP 515-565). Images were recorded onto a DVD at 30 frames per second with a high-sensitivity EBCCD (Electron Bombarded Charge-Coupled Device) camera (Hamamatsu Photonics, Shizuoka, Japan) and analyzed with the image-processing software ImageJ (National Institute of Mental Health, MD, USA). Based on the observation of time-successive images, the distribution of the long-axis length of DNA in solution was evaluated, where 40-70 DNA molecules were measured at each experimental condition.

C. AFM observation

For AFM imaging using an SPM-9700 (Shimadzu, Kyoto, Japan), 0.2 μM T4 DNA was dissolved in 10 mM Tris-HCl buffer solution at *p*H 7.5 with various concentrations of polyamines. The DNA solution was incubated for more than 10 min and then transferred onto a freshly cleaved mica surface.[37,42–46] We found that giant double-stranded DNA molecules tend to be adsorbed on the surface relatively easily in contrast to the adsorption of short DNA or single-stranded DNA molecules. Therefore, in the present study, the mica surface was not pretreated with any cationic species. After it was allowed to stand for 10 min at room temperature (25 °C), the mica was rinsed with water and dried under nitrogen gas. All measurements were performed in air using the tapping mode. The cantilever, OMCL-AC200TS-C2 (Olympus, Tokyo, Japan), was 200 μm long with a spring constant of 9-20 N/m. The scanning rate was 0.4 Hz and images were captured using the height mode in a 512 × 512 pixel format. The obtained images were plane-fitted and flattened by the computer program supplied with the imaging module. As a control, an AFM image of T4 DNA at a low concentration of SPD is shown in Fig. S1 of the supplementary material.

D. CD measurements

CD spectra of CT DNA upon the addition of polyamines were measured at 25 °C in 10 mM Tris−HCl buffer (*p*H 7.5) on a J-720W spectropolarimeter (JASCO, Tokyo, Japan). The DNA concentration was 30 μM in nucleotide units. Polyamine concentrations were varied from 1 to 500 μM. The cell path length was 1 cm. Data were collected every 1 nm between 220 and 340 nm at a scan rate of 200 nm/min, and were accumulated 3 times.

III. RESULTS

The left side of Fig. 1 shows the structural changes of individual T4 DNA molecules in the presence of various concentrations of 3(3)(3)4. In these images, single DNA molecules

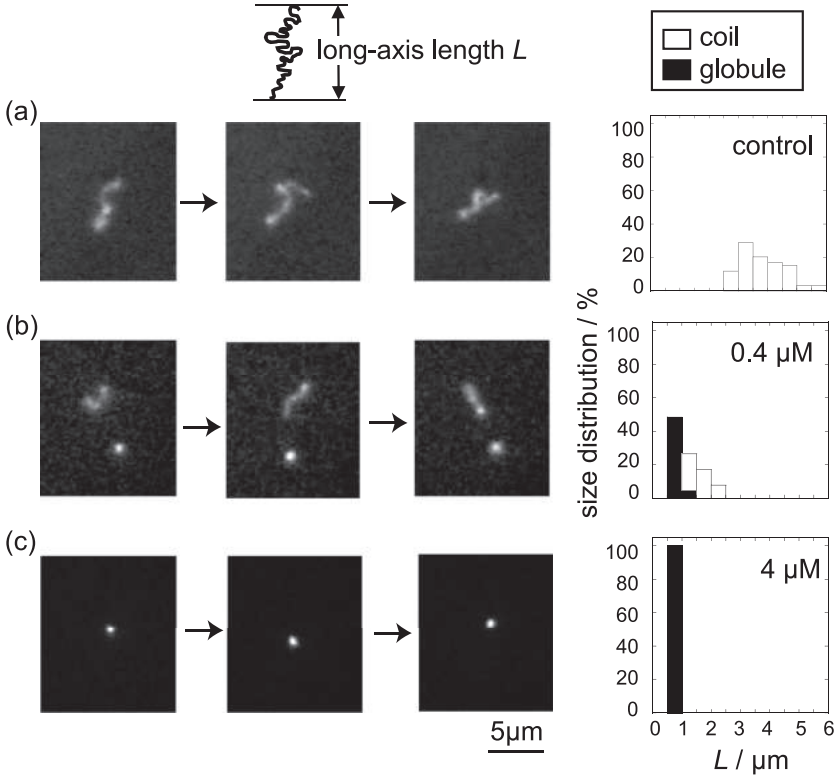

FIG. 1. (left) Real-time monitoring of single T4 DNA molecules in bulk solution at various concentrations of 3(3)(3)4: (a) 0 μM, (b) 0.4 μM, and (c) 4 μM. The total observation time is 3 s for (a)-(c). (right) Histograms of the long-axis length L for the corresponding concentrations of 3(3)(3)4.

undergo translational and intramolecular Brownian motion in bulk solution under FM observation. The right side of Fig. 1 shows the distribution of the long-axis length L of DNA together with an assignment of the conformational characteristics in FM images. In the absence of 3(3)(3)4, an elongated random coil conformation is observed (Fig. 1(a)). Figure 1(b) shows the coexistence of the coil and compact globule states upon the addition of 3(3)(3)4. With a further increase in the 3(3)(3)4 concentration, DNA folds into a compact globule state (Fig. 1(c)).

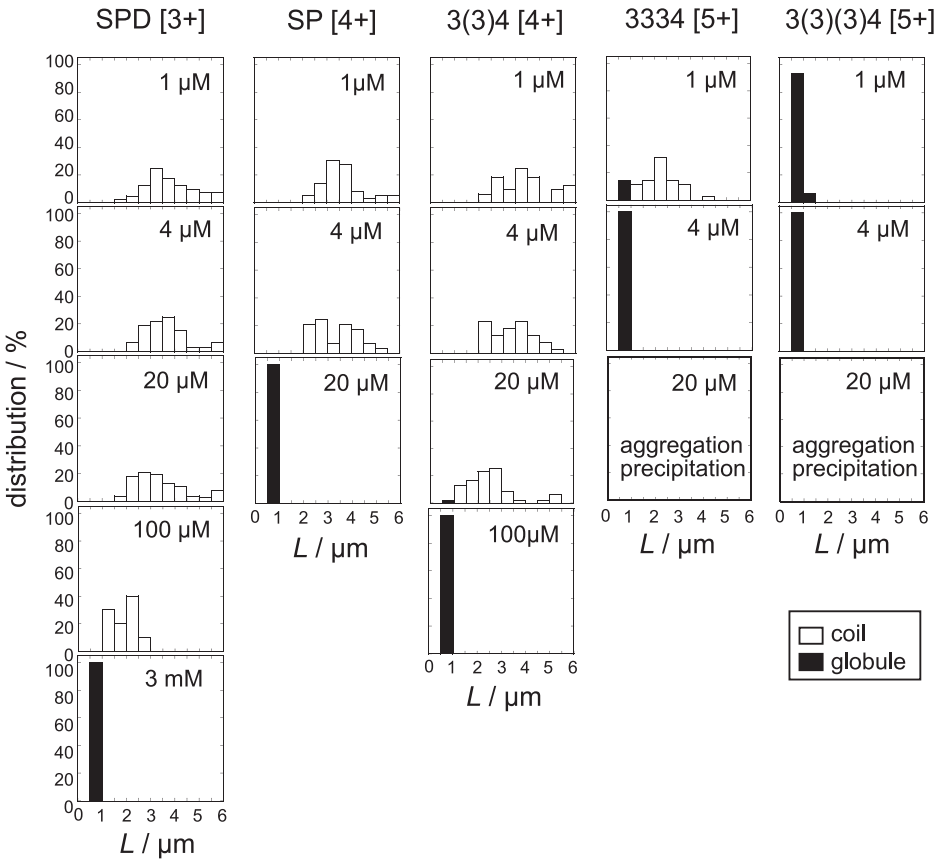

FIG. 2. Distribution of the long-axis length L of T4 DNA in solution at various polyamine concentrations. The DNA concentration is 0.1 μM in nucleotide units.

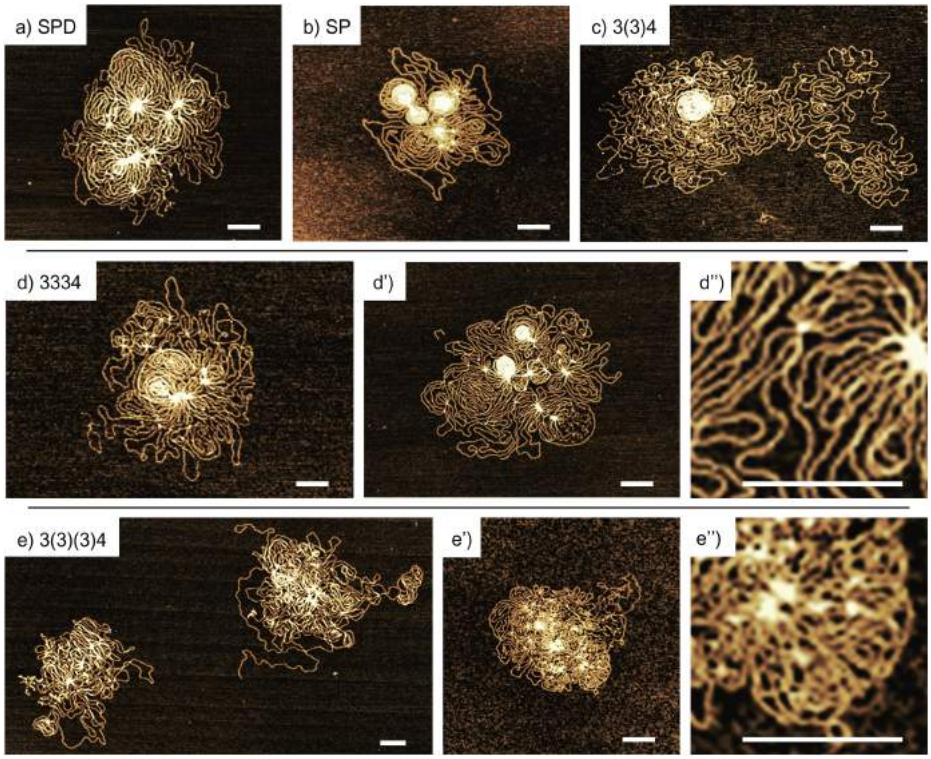

FIG. 3. AFM images of T4 DNA in the presence of various concentrations of polyamines: (a) 500 μM; (b) 10 μM; (c) 10 μM; (d) 2 μM; (d′) 5 μM; (e) 1.6 μM and (e′) 3 μM. (d″) and (e″) are magnified images of (d′) and (e′), respectively. Scale bar is 0.2 μm. All specimens were gently adsorbed on the flattened mica surface without shear stress. The DNA concentration is 0.2 μM in nucleotide units.

Figure 2 shows the histograms of the long-axis length,*L*, of DNA as the function of concentration of polyamines together with an assignment of the conformational characteristics in FM images. As shown in Fig. 2, polyamines with a larger number of amino groups have higher potentiality to induce DNA compaction. This experimental trend regarding the potency for DNA compaction corresponds well to observations in past studies.[10,27] Regarding the difference between linear- and branched-chain polyamines with four amino groups, SP is more potent than 3(3)4, i.e., the linear polyamine has a stronger effect than the branched polyamine. In contrast, pentavalent 3(3)(3)4 causes compaction at lower concentrations than 3334, i.e., the branched polyamine has a stronger effect than the linear-chain polyamine. This is attributed to the greater basicity of the quaternary ammonium group in 3(3)(3)4.

Figure 3 shows typical AFM images of DNA in the presence of linear- or branched-chain polyamines on a mica surface. The mica surface was not pretreated with any polycations such as magnesium or SP before the application of a droplet of sample. With the addition of a linear-chain polyamine, SPD, SP, or 3334, a multiple-looped structure appears on a two-dimensional surface (Figs. 3(a), 3(b), and 3(d′) together with its magnified image Fig. 3(d″)). The magnified image in Fig. 3(d″) clearly indicates the existence of a parallel ordering structure. The appearance of parallel ordering before compaction/condensation has been reported in previous studies.[37,42,43,45] On the other hand, this feature is not found with branched-chain polyamine-induced structures, where DNA segments tend to be oriented randomly with respect to each other (Figs. 3(c), 3(e), and 3(e′)). Especially, in the 3(3)(3)4-induced structure, a high-magnification AFM image clearly indicates the appearance of a crosslinked meshwork profile (Fig. 3(e″)). Additional AFM images are shown in the supplementary material to help clarify the differences in the effects of linear- and branched-chain polyamines (Fig. S2 of the supplementary material).

Figure 4 shows the CD spectra of DNA with the addition of different concentrations of polyamines, where calf thymus DNA was adopted for the measurements. For SPD and SP, there seems to be no apparent change in the CD spectra, indicating that the secondary structure retains the B-form under the present conditions. The branched-chain [4+] polyamine, 3(3)4, and the linear-chain [5+] polyamine, 3334, caused minimum changes in the CD spectrum. On the other hand, the branched-chain [5+] polyamine, 3(3)(3)4, induced a characteristic change in the DNA secondary structure. A marked increase of the positive Cotton effect at 278 nm was observed, which implies a transition in the secondary structure from the B-form to A-form (Fig. 4(e)).[47] Further addition of 3(3)(3)4 led to the appearance of the C-form, i.e., a decrease in the positive Cotton effect at 278 nm.[47] To better understand the changes in the CD spectrum induced by an increase in the polyamine concentration in a quantitative manner, we calculated the difference in ellipticity at 278 nm ($\Delta\theta$) between in the absence of a polyamine (θ_0) and at a concentration of r (θ_r), as defined by the following equation:

$$\Delta\theta = (\theta_r - \theta_0)\,. \tag{1}$$

The change in $\Delta\theta$ (mdeg) at 278 nm depending on the polyamine concentration is depicted in Fig. 5, which shows a marked change in CD with the addition of 3(3)(3)4. The minimum effect of the linear polyamines, SPD and SP, indicates that the secondary structure retains the B-form under the present conditions. This result is consistent with those

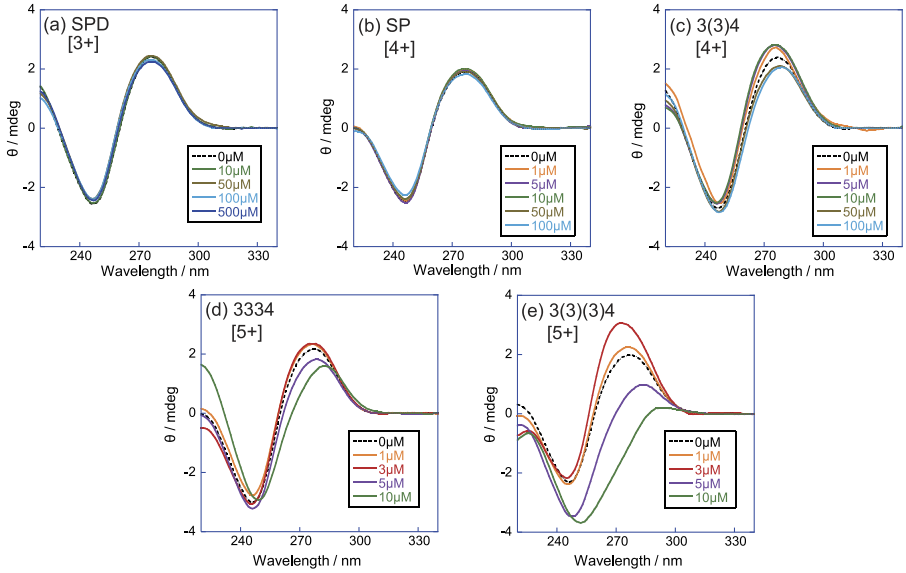

FIG. 4. CD spectra of calf thymus (CT) DNA at different concentrations of polyamines: (a) SPD; (b) SP; (c) 3(3)4; (d) 3334, and (e) 3(3)(3)4. The concentration of CT DNA is 30 μM in nucleotide units.

in previous studies.[41,42] Gosule and Schellman showed that the B-form of DNA was preserved upon the addition of an excess amount of SP.[48] Ouameur and Tajmir-Riahi reported that neither putrescine, SPD, nor SP dramatically affected the B-form of DNA.[49] Whereas these studies showed that linear polyamines had only minute effects on the secondary structure of DNA, Thomas *et al.* found that a B-A transition could be efficiently induced by the addition of SP to a DNA oligomer (41 bases) with a specific sequence of estrogen response element.[50] It has also been reported that polyamines cause a B-A transition only in solutions with a high level of ethanol.[51,52] Interestingly, the present results in Figs. 4 and 5 indicate that branched-chain polyamines cause a B-A transition for random sequence CT DNA in the usual aqueous environment.

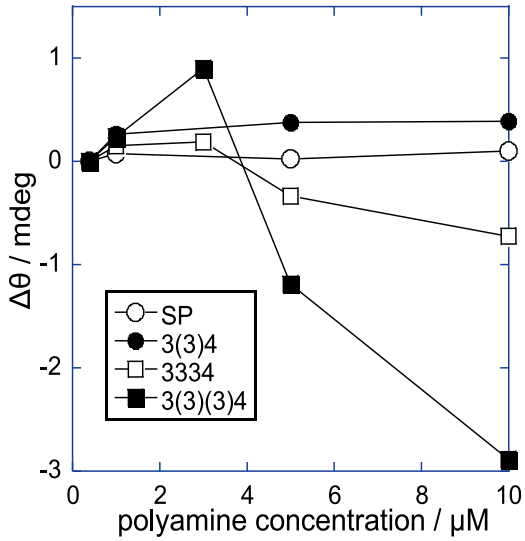

FIG. 5. Plots of $\Delta\theta$ at 278 nm vs. polyamine concentration. $\Delta\theta = (\theta_r - \theta_0)$, where θ_0 corresponds to the state in the absence of polyamine. The concentration of CT DNA was 30 μM in nucleotide units.

IV. DISCUSSION

The results of AFM observations show different effects of linear- and branched-chain polyamines on the overall morphology of long DNA molecules as shown in Fig. 3. Here, we discuss the characteristic features in AFM images. To evaluate the degree of parallel alignment observed by AFM in a quantitative manner, we analysed the change in conformation by considering the difference in the angles between nearby segments. The procedure used for the analysis is depicted in Fig. 6. We arbitrarily choose a straight line on an AFM image and determined the angle differences between neighboring DNA segments,

$$\Delta\phi_i = (\phi_{i+1} - \phi_i)\,. \tag{2}$$

We adopted $\cos 2\Delta\phi_i$ as a measure of the parallel ordering between neighboring DNA segments in two dimensions.[37] The order parameter S was then calculated as the ensemble average above 50 data points for each DNA molecule using the equation

$$S = \langle \cos 2\Delta\phi_i \rangle\,, \tag{3}$$

where the ensemble average was deduced from the angle differences, $\Delta\phi_i$, along multiple straight lines with different orientations on the AFM images. For this analysis, we considered more than 10 lines with a random orientation on the AFM image of individual DNA molecules. The crossing angle is within the range $0 \le \Delta\phi_i \le \pi/2$, which has been usually adapted in evaluating a 2D order parameter in a liquid crystal.[53] Here, it is noted that $S = 0$ corresponds to isotropic phase and $S = 1$ to the fully aligned phase. The lower panel in Fig. 6 shows the change in the order parameter S with different polyamines for the corresponding AFM pictures given in Fig. 3. To evaluate the effective shrinkage of DNA in the presence of polyamines, we also calculated the average segment density by adopting the inverse of the lengths $(1/L)$ between the segments on the same straight lines that were used to determine the angle differences. Based on the parameter $1/L$, the degree of shrinkage of DNA appears to be essentially the same. Thus, it has become clear that the order parameter S exhibits

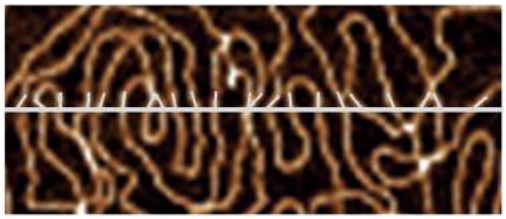

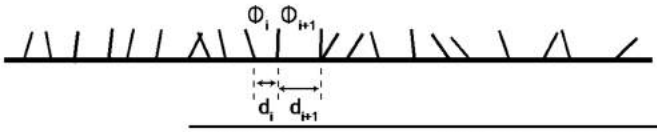

$$\Delta\phi_i = \phi_{i+1} - \phi_i$$
$$S = \langle \cos 2\Delta\phi_i \rangle$$
$$L = \langle d_i \rangle$$

AFM image in Fig. 3	Polyamine	Ordering: S	Density: $1/L$ [$\times 10^{-2}$nm^{-1}]
a	SPD	0.59±0.07	5.0±0.7
b	SP	0.57±0.08	4.3±0.3
c	3(3)4	0.39±0.08	4.8±0.5
d′	3334	0.51±0.08	5.0±0.6
e′	3(3)(3)4	0.23±0.08	7.1±1.1

FIG. 6. Schematic representation of the procedure used to evaluate the order parameter S and the density $1/L$ from AFM images. S and $1/L$ are calculated from the equations $S = \langle \cos 2\Delta\phi_i \rangle$ and $L = d_i$, where $\langle * \rangle$ is the ensemble average. The lower table shows S and $1/L$ based on the AFM images in Figs. 3(a)–3(c), 3(d′), and 3(e′).

a significant difference between linear- and branched-chain polyamines. The ordering in the presence of 3(3)4 and 3(3)(3)4 is rather small, which corresponds to the observation of the formation of a mesh-like structure.

Next, we discuss why branched-chain polyamines tend to form the mesh-like structure on the long DNA. Under the framework of counter ion condensation theory for a stiff rod-like polyelectrolyte chain,[54,55] negative phosphate groups along a double-stranded DNA are shielded by up to ca. 90%, 92%, and 95% in response to the addition of [3+], [4+], and [5+] ions, respectively, in aqueous solution with a dielectric constant, or a relative permittivity of 80 at around 300 K. In other words, 5%-10% of the negative charges still survive just before the folding transition, whereas almost all of the negative charges disappear after the folding transition to the compact state due to the absorption of additional cations in the vicinity of the double-stranded structure. In relation to the effect of polycation below the concentration to induce DNA compaction, Ouameur and Tajmir-Riahi[49] evaluated the binding of linear polyamines onto double-stranded DNA through a systematic spectroscopic study together with electrophoresis and confirmed a decrease in the negative charge in accordance with counter ion condensation theory.[54,55] Thus, the enhancement of parallel alignment just before compaction by linear-chain polyamines is attributed to the self-avoiding volume interaction between DNA segments due to the surviving negative charges along the double-stranded structure (Fig. 7(a)), under a shrinking effect with a partially segregated sate. Note that DNA behaves as stiff rods on a length-scale below its persistence length of 40-50 nm. Linear polyamines are expected to bind to the double-stranded structure by taking a nearly parallel conformation.[56,57] It should be noted that the counter ion condensation theory[54,55] applies to isolated rod-like strong polyelectrolytes, as in short oligomeric DNA, and that this theory does not interpret in a correct manner on the large discrete change of the behavior of the counter ions accompanied by the folding transition of long DNA as has been adopted in the present study. For branched-chain polyamines, it is expected that a branching positive-charged group may promote binding with other segments. Especially, the high basicity of a quaternary ammonium group, as in 3(3)(3)4, is expected to promote the potentiality to bridge DNA segments even under the condition where several percent of the negative charge survives along the double-stranded structure (Fig. 7(b)).

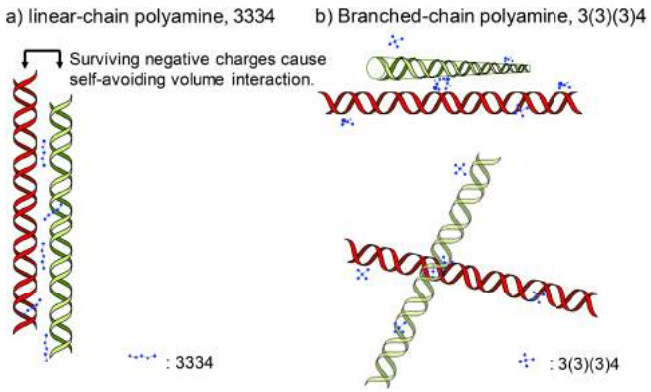

FIG. 7. Schematic illustration of different modes of interaction between double-stranded DNA and polyamines just before compaction. (a) Self-avoiding volume interaction between DNA segments induces parallel alignment; (b) high basicity of 3(3)(3)4 promotes "bridging" of DNA segments even when repulsive negative charge survives.

We may thus explain the appearance of a mesh-like structure just before full compaction in terms of the bridging effect of the branched moiety of polyamines. It is also noted that the branched-chain polyamines 3(3)(3)4 lead to the alteration of the DNA secondary structure from the B-form to A-form (Fig. 4). The above consideration suggests that the unique features observed by AFM are closely related to the changes in the secondary structure of DNA.

V. CONCLUSION

The present study revealed the characteristic properties of branched-chain polyamines from a physico-chemical point

of view. Branched-chain polyamines tend to cause bridging between segments in a giant DNA and then induce a meshwork assembly of randomly oriented DNA fibers. On the other hand, linear-chain polyamines preferentially induce linear alignment to form multiple-looped structures. The specific effect of branched-chain polyamines was also noted in the observation of the secondary structure of DNA by CD spectroscopy: a transition from a B- to A-form. There is interplay between the higher-order and secondary structures of DNA. As a future extension of this study, it may be important to clarify the biological significance of the role of branched-chain polyamines in hyperthermophiles in relation to their effects on both the higher-order and secondary structures of DNA.

SUPPLEMENTARY MATERIAL

See supplementary material for the synthesis of polyamines and the additional examples of AFM images.

ACKNOWLEDGMENTS

This work was partly supported by KAKENHI, Grants-in-Aid for Scientific Research Nos. 15H02121 and 25103012 to K.Y., 15K08027 to N.U., 26292045 to S.F., and 25390038 to Y.Y.

[1] C. W. Tabor and H. Tabor, Annu. Rev. Biochem. **53**, 749 (1984).
[2] L. C. Gosule and J. A. Schellman, Nature **259**, 333 (1976).
[3] D. K. Chattoraj, L. C. Gosule, and J. A. Schellman, J. Mol. Biol. **121**, 327 (1978).
[4] I. Baeza, P. Gariglio, L. M. Rangel, P. Chavez, L. Cervantes, C. Arguello, C. Wong, and C. Montanez, Biochemistry **26**, 6387 (1987).
[5] M. Takahashi, K. Yoshikawa, V. V. Vasilevskaya, and A. R. Khokhlov, J. Phys. Chem. B **101**, 9396 (1997).
[6] Y. Yoshikawa, K. Yoshikawa, and T. Kanbe, Langmuir **15**, 4085 (1999).
[7] M. Saminathan, T. Thomas, A. Shirahata, C. K. Pillai, and T. J. Thomas, Nucleic Acids Res. **30**, 3722 (2002).
[8] T. J. Thomas, H. A. Tajmir-Riahi, and T. Thomas, Amino Acids **48**, 2423 (2016).
[9] V. A. Bloomfield, Biopolymers **31**, 1471 (1991).
[10] V. A. Bloomfield, Biopolymers **44**, 269 (1997).
[11] J. DeRouchey, V. A. Parsegian, and D. C. Rau, Biophys. J. **99**, 2608 (2010).
[12] A. Estevez-Torres and D. Baigl, Soft Matter **7**, 6746 (2011).
[13] J. DeRouchey and D. C. Rau, Biochemistry **52**, 3000 (2013).
[14] H. S. Basu, H. C. Schwietert, B. G. Feuerstein, and L. J. Marton, Biochem. J. **269**, 329 (1990).
[15] V. Vijayanathan, T. Thomas, A. Shirahata, and T. J. Thomas, Biochemistry **40**, 13644 (2001).
[16] S. Prevost, S. Riemer, W. Fischer, R. Haag, C. Bottcher, J. Gummel, I. Grillo, M.-S. Appavou, and M. Gradzielski, Biomacromolecules **12**, 4272 (2011).
[17] M. An, S. R. Parkin, and J. E. DeRouchey, Soft Matter **10**, 590 (2014).
[18] A. Venancio-Marques, A. Bergen, C. Rossi-Gendron, S. Rudiuk, and D. Baigl, ACS Nano **8**, 3654 (2014).
[19] E. Grueso, E. Kuliszewska, E. Roldan, P. Perez-Tejeda, R. Prado-Gotor, and L. Brecker, RSC Adv. **5**, 29433 (2015).
[20] N. Umezawa, Y. Horai, Y. Imamura, M. Kawakubo, M. Nakahira, N. Kato, A. Muramatsu, Y. Yoshikawa, K. Yoshikawa, and T. Higuchi, ChemBioChem **16**, 1811 (2015).
[21] Y. Yoshikawa and K. Yoshikawa, FEBS Lett. **361**, 277 (1995).
[22] I. Nayvelt, M. T. Hyvonen, I. Alhonen, I. Pandya, T. Thomas, A. R. Khomutov, J. Vepsalainen, R. Patel, T. A. Keinanen, and T. J. Thomas, Biomacromolecules **11**, 97 (2010).
[23] Y. Yoshikawa, N. Umezawa, Y. Imamura, T. Kanbe, N. Kato, K. Yoshikawa, T. Imanaka, and T. Higuchi, Angew. Chem., Int. Ed. **52**, 3712 (2013).
[24] V. A. Bloomfield, Curr. Opin. Struct. Biol. **6**, 334 (1996).
[25] J. Pelta, F. Livolant, and J. L. Sikorav, J. Biol. Chem. **271**, 5656 (1996).
[26] E. Raspaud, M. Olvera de la Cruz, J. L. Sikorav, and F. Livolant, Biophys. J. **74**, 381 (1998).
[27] K. Yoshikawa and Y. Yoshikawa, *Pharmaceutical Perspectives of Nucleic Acid-Based Therapeutics* (Taylor & Francis, Oxford, 2002), pp. 136–163.
[28] Y. Burak, G. Ariel, and D. Andelman, Biophys. J. **85**, 2100 (2003).
[29] H. Schiessel, J. Phys.: Condens. Matter **15**, R699 (2003).
[30] N. V. Hud and I. D. Vilfan, Ann. Rev. Biophys. Biomol. Struct. **34**, 295 (2005).
[31] K. Besteman, K. van Eijk, and S. G. Lemay, Nat. Phys. **3**, 641 (2007).
[32] B. A. Todd and D. C. Rau, Nucleic Acids Res. **36**, 501 (2008).
[33] V. B. Teif and K. Bohinc, Prog. Biophys. Mol. Biol. **105**, 208 (2011).
[34] M. Ueda and K. Yoshikawa, Phys. Rev. Lett. **77**, 2133 (1996).
[35] T. Akitaya, A. Seno, T. Nakai, N. Hazemoto, S. Murata, and K. Yoshikawa, Biomacromolecules **8**, 273 (2007).
[36] Y. T. Sato, S. N. Watanabe, T. Kenmotsu, M. Ichikawa, Y. Yoshikawa, J. Teramoto, T. Imanaka, A. Ishihama, and K. Yoshikawa, Biophys. J. **105**, 1037 (2013).
[37] Y. Yoshikawa, Y. Suzuki, K. Yamada, W. Fukuda, K. Yoshikawa, K. Takeyasu, and T. Imanaka, J. Chem. Phys. **135**, 225101 (2011).
[38] Y. Terui, M. Ohnuma, K. Hiraga, E. Kawashima, and T. Oshima, Biochem. J. **388**, 427 (2005).
[39] T. Oshima, Amino Acids **33**, 367 (2007).
[40] N. Morimoto, W. Fukuda, N. Nakajima, T. Masuda, Y. Terui, T. Kanai, T. Oshima, T. Imanaka, and S. Fujiwara, J. Bacteriol. **192**, 4991 (2010).
[41] K. Okada, R. Hidese, W. Fukuda, M. Niitsu, K. Takao, Y. Horai, N. Umezawa, T. Higuchi, T. Oshima, Y. Yoshikawa, T. Imanaka, and S. Fujiwara, J. Bacteriol. **196**, 1866 (2014).
[42] Y. Fang and J. H. Hoh, J. Am. Chem. Soc. **120**, 8903 (1998).
[43] Y. T. A. Chim, J. K. W. Lam, Y. Ma, S. P. Armes, A. L. Lewis, C. J. Roberts, S. Stolnik, S. J. B. Tendler, and M. C. Davies, Langmuir **21**, 3591 (2005).
[44] A. Podesta, M. Indrieri, D. Brogioli, G. S. Manning, P. Milani, R. Guerra, L. Finzi, and D. Dunlap, Biophys. J. **89**, 2558 (2005).
[45] K. Besteman, K. van Eijk, I. D. Vilfan, U. Ziese, and S. G. Lemay, Biopolymers **87**, 141 (2007).
[46] L. Hamon, D. Pastre, P. Dupaigne, C. L. Breton, E. L. Cam, and O. Pietrement, Nucleic Acids Res. **35**, e58 (2007).
[47] V. I. Ivanov, L. E. Minchenkova, A. K. Schyolkina, and A. I. Poletayev, Biopolymers **12**, 89 (1973).
[48] L. C. Gosule and J. A. Schellman, J. Mol. Biol. **121**, 311 (1978).
[49] A. A. Ouameur and H. A. Tajmir-Riahi, J. Biol. Chem. **279**, 42041 (2004).
[50] T. Thomas, G. D. Kulkarni, M. A. Gallo, N. Greenfield, J. S. Lewis, A. Shirahata, and T. J. Thomas, Nucleic Acid Res. **25**, 2396 (1997).
[51] E. E. Minyat, V. I. Ivanov, A. M. Kritzyn, L. E. Minchenkova, and A. K. Schylokina, J. Mol. Biol. **128**, 397 (1978).
[52] S. Hormeno, F. Moreno-Herrero, B. Ibarra, J. L. Carrascosa, J. M. Valpuesta, and J. R. Arias-Gonzalez, Biophys. J. **100**, 2006 (2011).
[53] D. Frenkel and R. Eppenga, Phys. Rev. A **31**, 1776–1787 (1985).
[54] F. Oosawa, Biopolymers **9**, 677 (1970).
[55] G. S. Manning, Q. Rev. Biophys. **11**, 179 (1978).
[56] I. S. Tolokh, S. A. Pabit, A. M. Katz, Y. Chen, A. Drozdetski, N. Baker, L. Pollack, and A. V. Onufriev, Nucleic Acids Res. **42**, 10823 (2014).
[57] A. V. Drozdetski, I. S. Tolokh, L. Pollack, N. Baker, and A. V. Onufriev, Phys. Rev. Lett. **117**, 028101 (2016).